Global Traveling Wave Triggered by Local Phase Slips

Kunihiko Kaneko
Department of Pure and Applied Sciences, University of Tokyo, Komaba, Tokyo 153, Japan
(Received 15 October 1991)

A novel type of traveling-wave attractor is found in coupled-map lattices. Attractors with different velocities coexist, which are coded by the asymmetry of the wave form. Admissible velocities for the attractors form a series of bands. The velocity is proportional to the winding number of phase slips. If the wavelength and the system size do not match, the wave is modulated by low-dimensional chaos, which leads to spontaneous velocity switching by frustration or reverse transmission of chaotic modulation.

PACS numbers: 05.45.+b, 47.25.Ae

Spatiotemporal chaos has recently been studied in many fields, including Bénard convection experiments, Josephson-junction arrays, charge-density waves, optical turbulence, chemical reaction-diffusion systems, excitable media in biological systems, and so on. Several years ago, the author proposed a coupled-map lattice (CML), which provides a novel standard model for the study of spatiotemporal chaos [1-5]. A CML is a discrete-spacetime dynamics, consisting of successive parallel procedures. A typical example adopts local chaos by the logistic map and spatial diffusion [1], given by

$$x_{n+1}(i)=(1-\epsilon)f(x_n(i)) + \tfrac{1}{2}\epsilon[f(x_n(i+1))+f(x_n(i-1))] \quad (1)$$

with $f(y)=1-ay^2$. The lattice site i takes values from 1 to N, the system size [6]. The model has clarified some novel classes of phenomenology in spatiotemporal chaos, such as spatial bifurcation, frozen random chaos, pattern selection with suppression of chaos, spatiotemporal intermittency, and quasistationary supertransients [1-4]. No example of a traveling-wave structure is known in the weak-coupling regime ($\epsilon \leq 0.4$), in contrast to experimental observations of traveling waves in spatially extended systems [7].

In the present Letter, we report the discovery of a novel class of traveling-wave attractors in the model (1) in the strong-coupling regime. This traveling wave is maintained by a local phase slip (a unit of 2π phase advance), which influences all lattice points (and is thus global). The velocities of the attractors fall on admissible bands, determined by the number of such phase slips. Spontaneous velocity switching due to chaos is also found, arising from the frustration by the mismatch of a selected wave number with the system size.

In our model (1), regular patterns with a certain wavelength are selected with the suppression of chaos, in the medium nonlinearity regime ($1.55 < a < 1.75$). The regular patterns are fixed in time in the weak-coupling case [2], while attractors with a regular traveling wave can be found in the strong-coupling case. Examples of attractors are given in Fig. 1. Besides an attractor with a frozen pattern, there are attractors with a moving pattern forming a traveling wave. The selected velocity here is very slow, on the order of 10^{-3} site per step. The emergence of such slow dynamics is rather surprising, since the original logistic map does not involve such a long time scale. Attractors with different velocities coexist (see Fig. 1). Admissible velocities lie in small bands located at 0, $\pm v_1$, $\pm v_2(\approx 2v_1)$, and $\pm v_3(\approx 3v_1)$. For example, $v_1=1.3\times10^{-3}$, $v_2=2.75\times10^{-3}$, and $v_3=4.1\times10^{-3}$, for $a=1.71$, $\epsilon=0.5$, and $N=50$. Numerically, v_k is approximately proportional to k [8,9].

To understand the mechanism of this velocity selection, we note that $x_n(i)$ oscillates in time. One can assign a phase of oscillation to a lattice site i relative to $(x_n(i),x_n(i+1))$. When there is phase change of 2π between sites i and $i+l$, it is numerically found that this interval unit $[i,i+l]$ maintains the traveling wave. For example, in the attractor with velocity v_1 in Fig. 1, the oscillation is close to period 4, with slow quasiperiodic modulation. It is possible to assign a phase change $m\pi/2$ ($m=\pm1$) between a lattice site i and a lattice site $i+j$ in a neighboring domain, according to the order of the

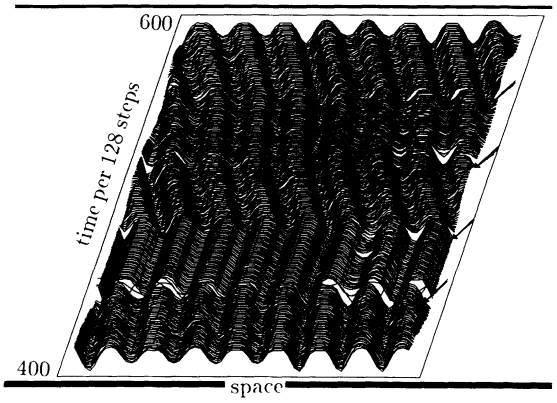

FIG. 1. Amplitude-space plot of $x_n(i)$ with a shift of time steps. 200 sequential patterns $x_n(i)$ are shown with time (per 64 steps), after discarding 25600 initial transients, starting from a random initial condition. $a=1.71$, $\epsilon=0.5$, and $N=64$. In order to see four attractors, an input is added, at the time step and the lattice point indicated by an arrow, to switch among attractors. The input is added so that the value of $x_n(i)$ at the corresponding i,n is shifted to 1.0. The velocities are switched as $v=0$, $v=-v_1$, $v=v_1$, and $v=v_2$.

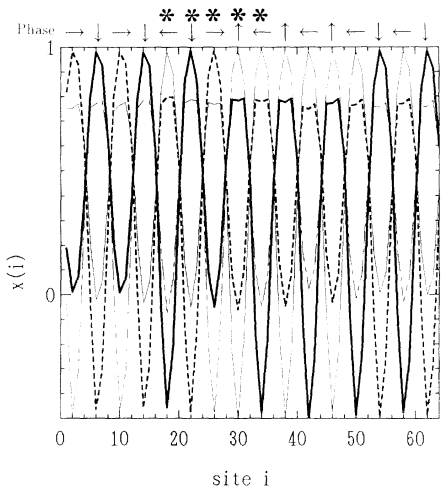

FIG. 2. Amplitude-space plot: Plotted are four sequential patterns $x_n(i)$, in the order of thin line ($n=10001$), thick line ($n=10002$), thick dashed line ($n=10003$), and dashed line ($n=10004$). $a=1.72$, $\epsilon=0.5$, and $N=64$. A negative trigger exists (shown by the asterisks), and the velocity is $-v_i$.

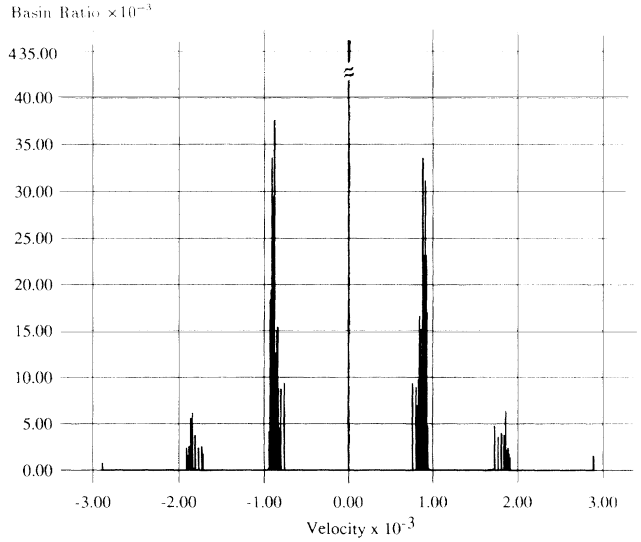

FIG. 3. Histogram of the basin ratio for traveling waves as a function of velocity for $a=1.73$, $N=50$, and $\epsilon=0.5$. Velocities of attractors are examined, from 10^5 steps after discarding 10^5 initial transients. The histogram is obtained by sampling velocities over 5000 randomly chosen initial conditions.

period-4-like motion. Under the periodic boundary condition, the total phase change should be $2M\pi$. The velocity is found to be exactly zero for an attractor with $M=0$. If $M=1$, there must be a sequence of five domains with phases 0, $\pi/2$, π, $3\pi/2$, 2π with an increase of lattice site i (Fig. 2). This unit is a (positive) phase slip. A negative phase slip is defined by the mirror-symmetric pattern of the positive one. Numerically it is confirmed that the velocity of an attractor of winding number M with phase change $2M\pi$ (i.e., M is the number of positive phase slips minus the negative ones) falls on the velocity band v_M.

Since a phase slip is localized in space, one might think that the movement is a local phenomenon like soliton propagation. This is not the case. In the present case, this slip must pull all other regions to make them travel, changing the phases of oscillations of all lattice points. Thus a local phase slip globally influences all lattice points. Our dynamics gives a connection between local and global dynamics. One clear manifestation of the global aspect is the additivity of velocity. In our system, the velocity of the wave is proportional to the winding number. This proportionality gives a clear distinction between our dynamics and soliton-type dynamics, where, of course, the speed of a soliton does not increase with the number of solitons present.

In Fig. 3, we have measured the basin volume ratio for attractors of different velocities. The band structure of admissible velocities is found. In each band there are discrete sets of admissible velocities. The number of attractors is large, since there are many admissible velocities in each band. The basin volume for an attractor decreases rapidly with an increase of the (band) velocity v_k. Although the velocity band is determined by the winding number, the difference of velocities within the same band is governed by the wave form, given by the configuration of domain patterns. To quantify the change of wave form we define the spatial asymmetry by $s\equiv\langle(1/N)\sum_{j=1}^{N}[x_n(j+1)-x_n(j)]^3\rangle$, with $\langle\cdots\rangle$ the long-time average. Since our model has a mirror symmetry, an attractor with a traveling wave must break the spatial symmetry, leading to $s\neq 0$. Here the velocity of an attractor is proportional to its asymmetry s, as plotted in Fig. 4. For an attractor with $v=0$, s is zero within numerical accuracy. Thus spatial symmetry is attained through the attraction to the non-traveling-wave attractor, starting from an initial condition with spatial asymmetry. Again, this spatial sym-

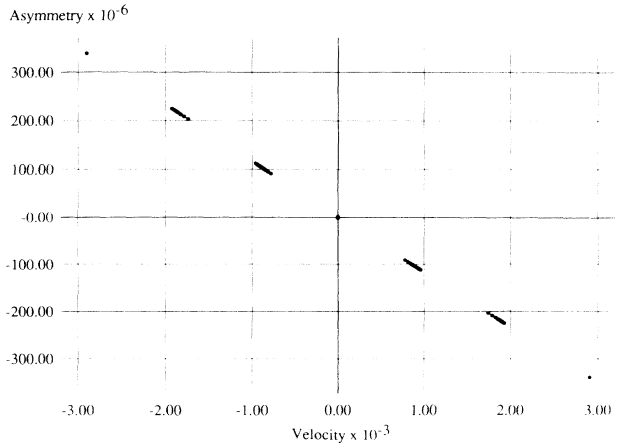

FIG. 4. Velocities of attractors vs asymmetry s, obtained from the data for Fig. 3.

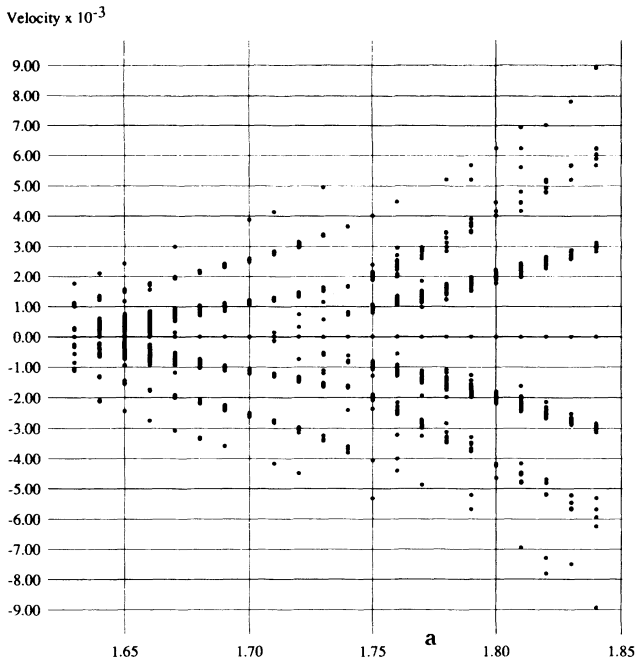

FIG. 5. Velocities of attractors obtained from 50000 steps after discarding 50000 initial transients. Velocities from 100 randomly chosen initial conditions are overlayed. $N=64$ and $\epsilon=0.5$.

metry is not a local but a global property. The asymmetry in each domain is canceled through the summation over the total lattice. This self-organized symmetry is possible only if there are traveling-wave attractors.

The dependence of the velocity v_p on the nonlinearity a is shown in Fig. 5, where the velocities are plotted obtained from 100 initial conditions, over $1.6 < a < 1.85$. The existence of distinct velocity bands is clearly seen. Both the velocities and the gaps between bands increase with the nonlinearity.

Since our system has a selected wavelength λ (≈ 8 in the examples here), the fractional part of N/λ is relevant to the nature of the traveling wave. If this fractional part is not close to 0.5, the motion is quasiperiodic for most sizes and parameters. To examine the dynamics of our attractors, Lyapunov spectra are measured [2]. Over parameter regime $1.65 < a < 1.85$ and for most sizes, the maximal exponent is zero, irrespective of the velocity of the attractors (see Fig. 6). The motion of the wave is quasiperiodic with complete elimination of chaos by the pattern selection. If chaos were not sufficiently eliminated, it would be impossible to sustain a spatially periodic pattern during the course of propagation. Such elimination of chaos is impossible for an arbitrary wave pattern, since our dynamics has topological chaos.

If there is mismatch between the system size and the wavelength (the fractional part of N/λ is near 0.5), any pattern with any velocity and wavelength has frustration. This frustration introduces remnant chaotic motion,

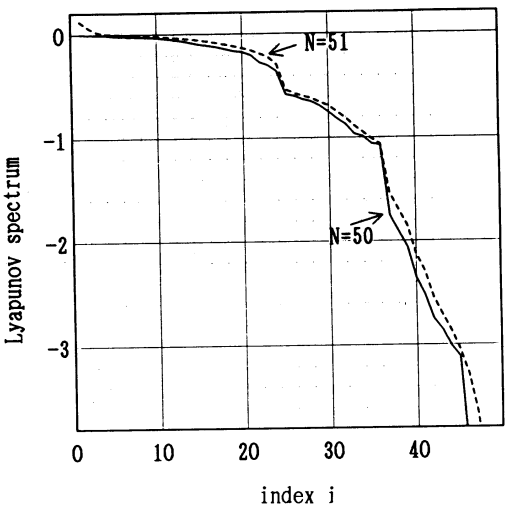

FIG. 6. Lyapunov spectra of our model with $a=1.69$ and $\epsilon=0.5$, for a traveling-wave attractor. The calculation is carried out through the products of Jacobi matrices over 32768 time steps, after discarding 50000 initial transients. $N=50$ (solid line) and $N=51$ (dashed line).

which leads to spontaneous switching among patterns with different velocities. In Fig. 7(a), the velocity spontaneously switches as 0, $-v_2$, $-v_1$, 0, v_1, $-v_1$, v_2, 0, successively. Here states with different velocities merge, which are disconnected attractors for most other sizes without frustration. This spontaneous switching arises from chaotic motion of each pattern, and provides a novel example of chaotic itinerancy [10]. For the switching, we need modulation of the wave. Indeed, each wave form starts to be rather irregular in advance of the switching. The wavelength, on the other hand, is not affected in the course of the switching process. The switching occurs through the change of phase of oscillations, leading to the creation or destruction of phase slips.

Lyapunov spectra of this frustration-induced floating wave are plotted in Fig. 6. Few (four in our simulation) exponents are positive. The chaos here is weak and low dimensional. The spectra have a plateau at the null exponent, implying the existence of a marginal mode for the traveling wave. This plateau is characteristic of a chaotic system with a traveling wave.

For a larger system size, such a floating pattern is hardly observed. The system settles down to a frozen or a traveling-wave pattern after long transients. Since the number of chaotic modes is few (~ 1), the frustration per degree of freedom decreases with N. The distortion due to the mismatch of phase is still there, but it is distributed over a large size and is too weak to switch the pattern. Instead, the remnant frustration leads to chaotic modulation of the wave, which propagates in the *opposite* direction from the traveling wave, as is shown in Fig. 7(b) for $a=1.69$ for $N=100$. The Lyapunov spectrum has few positive exponents and is almost flat near 0.

As has been reported [2], the traveling state is not ob-

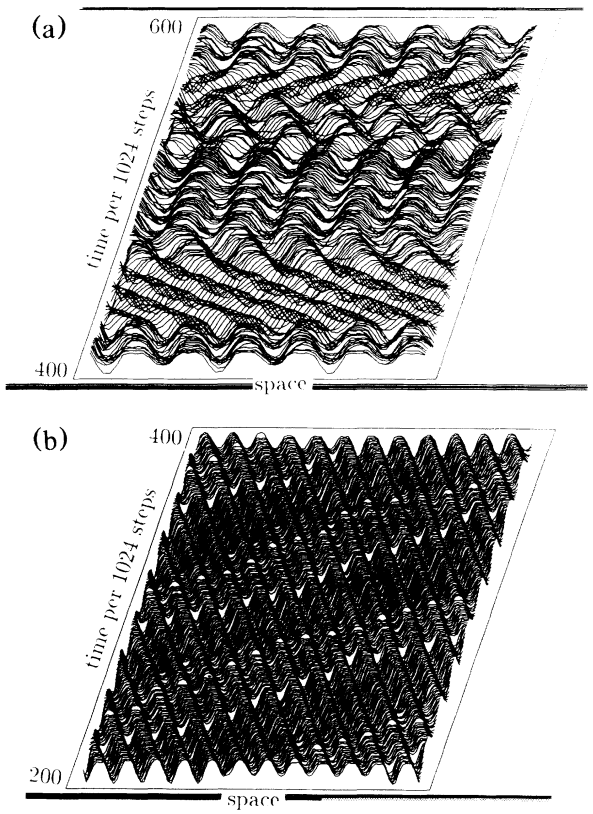

FIG. 7. Amplitude-space plot of $x_n(i)$ with a shift of time steps. 200 sequential patterns $x_n(i)$ are depicted with time (per 1024 times steps), after discarding 40960 initial transients, starting from a random initial condition. $a=1.69$, $\epsilon=0.5$. (a) $N=51$ and (b) $N=100$.

served for $\epsilon<\epsilon_c\approx 0.402$. We note that the velocity does not go to zero as ϵ approaches ϵ_c from above. For example, the velocity lies within $(1.0\text{–}1.8)\times 10^{-3}$ over $0.402<\epsilon<0.45$, for $N=50$ and $a=1.71$. Instead, the basin volume for such a traveling-wave attractor vanishes with $\epsilon\to\epsilon_c+0$, which is the reason why only frozen patterns are observed as attractors for $\epsilon<\epsilon_c$.

In the present Letter, we have reported the admissible velocity bands in the traveling wave triggered by phase slips. Although the phase slips are already found in partial differential equation (PDE) systems, the slips there do not bring about the traveling wave of the present type. The wave in PDE systems, so far, is governed by the frontal structure: A traveling wave for a PDE for $\phi(r,t)$ is given as a homoclinic orbit in the ordinary differential equation obtained under the assumption of the wave-form solution $\phi(r,t)=\mathrm{f}(r-vt)$. It is a future important problem to examine if a wave solution triggered by phase slips also exists in PDE systems.

In a weaker nonlinearity regime ($a<1.55$), chaos is not suppressed, and various sizes of domains coexist, which travel in one direction with fluctuation of domain boundaries. This state corresponds to the frozen random phase in the weaker-coupling regime [2].

Traveling waves have been observed in Bénard convection experiments [7], where the coexistence of attractors has not seriously been examined. It is important to check if attractors with different velocities coexist (with the application of perturbation), and to search for our phenomena.

Mismatch of the wavelength and the system size leads to remnant chaos. If chaos is strong, it leads to a frustration-induced floating wave. Our system itinerates over pseudostable states with different velocities. For a larger system size, chaos is reversely transmitted as modulation on the traveling wave. Experimental observations of such chaotic traveling waves are also expected.

I would like to thank K. Nemoto, K. Ikeda, and M. Sano for useful discussions. This work is partially supported by Grant-in-Aids for Scientific Research from the Ministry of Education, Science and Culture of Japan.

[1] K. Kaneko, Prog. Theor. Phys. **72**, 480 (1984); **74**, 1033 (1985); Prog. Theor. Phys. Suppl. **99**, 263 (1989); in *Formation, Dynamics, and Statistics of Patterns*, edited by K. Kawasaki *et al.* (World Scientific, Singapore, 1990), and references cited therein.

[2] K. Kaneko, Physica (Amsterdam) **23D**, 436 (1986); **34D**, 1 (1989); **36D**, 60 (1989).

[3] J. P. Crutchfield and K. Kaneko, *Directions in Chaos* (World Scientific, Singapore, 1987).

[4] J. D. Keeler and J. D. Farmer, Physica (Amsterdam) **23D**, 413 (1986); P. Grassberger and T. Schreiber, Physica (Amsterdam) **50D**, 177 (1991).

[5] I. Waller and R. Kapral, Phys. Rev. A **30**, 2047 (1984).

[6] Throughout the paper we use the periodic boundary condition.

[7] D. R. Ohlsen *et al.*, Phys. Rev. Lett. **65**, 1431 (1990); P. Kolodner, Phys. Rev. A **42**, 2475 (1990); D. Bensimon *et al.*, J. Fluid Mech. **217**, 441 (1990).

[8] One might argue that the velocity band is an artifact of the discreteness of spacetime in our model. This is not the case. Since the speed is very slow (the order of 10^{-3} site per step), it is impossible to imagine a mechanism to which our original discreteness (1 site per step) is relevant. To examine a possible effect of spatial discreteness, we have also simulated a CML with a longer range, following the method of Sec. 7.5 in [2]. With the increase of range, our attractor gets spatially much smoother, approaching a continuous-space limit. The obtained attractors again have admissible bands of velocities. Thus the discreteness in space is not relevant to the velocity band structure.

[9] Our traveling-wave attractors are stable against the addition of noise. We have also checked the effect of numerical error by changing the precision, and our results are insensitive to errors.

[10] K. Ikeda, K. Matsumoto, and K. Ohtsuka, Prog. Theor. Phys. Suppl. **99**, 295 (1989); I. Tsuda, in *Neurocomputers and Attention*, edited by A. V. Holden and V. I. Kryukov (Manchester Univ. Press, Manchester, 1990); K. Kaneko, Phys. Rev. Lett. **63**, 219 (1989); Physica (Amsterdam) **41D**, 38 (1990).